Visualizing the dynamics of p21$^{Waf1/Cip1}$ cyclin-dependent kinase inhibitor expression in living animals

Naoko Ohtani*†, Yuko Imamura*, Kimi Yamakoshi*, Fumiko Hirota‡, Rika Nakayama§, Yoshiaki Kubo¶, Naozumi Ishimaru¶, Akiko Takahashi*, Atsushi Hirao‖**, Takatsune Shimizu††, David J. Mann‡‡, Hideyuki Saya††, Yoshio Hayashi¶, Seiji Arase¶, Mitsuru Matsumoto‡, Kazuki Nakao§, and Eiji Hara*†

*Institute for Genome Research, ‡Institute for Enzyme Research, and ¶Institute of Health Biosciences, University of Tokushima, Tokushima 770-8503, Japan; §Center for Developmental Biology, RIKEN, Kobe 650-0047, Japan; ‖Cancer Research Institute, Kanazawa University, Kanazawa 920-0934, Japan; **CREST, Japan Science and Technology Agency, Tokyo 102-0075, Japan; ††Institute for Advanced Medical Research, Keio University School of Medicine, Tokyo 160-8582, Japan; and ‡‡Division of Cell and Molecular Biology, Imperial College London, London SW7 2AZ, United Kingdom

Communicated by Thaddeus P. Dryja, Harvard Medical School, Boston, MA, July 25, 2007 (received for review May 11, 2007)

Although the role of *p21$^{Waf1/Cip1}$* gene expression is well documented in various cell culture studies, its *in vivo* roles are poorly understood. To gain further insight into the role of *p21$^{Waf1/Cip1}$* gene expression *in vivo*, we attempted to visualize the dynamics of *p21$^{Waf1/Cip1}$* gene expression in living animals. In this study, we established a transgenic mice line (p21-*p*-luc) expressing the firefly luciferase under the control of the *p21$^{Waf1/Cip1}$* gene promoter. In conjunction with a noninvasive bioluminescent imaging technique, p21-*p*-luc mice enabled us to monitor the endogenous *p21$^{Waf1/Cip1}$* gene expression *in vivo*. By monitoring and quantifying the *p21$^{Waf1/Cip1}$* gene expression repeatedly in the same mouse throughout its entire lifespan, we were able to unveil the dynamics of *p21$^{Waf1/Cip1}$* gene expression in the aging process. We also applied this system to chemically induced skin carcinogenesis and found that the levels of *p21$^{Waf1/Cip1}$* gene expression rise dramatically in benign skin papillomas, suggesting that *p21$^{Waf1/Cip1}$* plays a preventative role(s) in skin tumor formation. Surprisingly, moreover, we found that the level of *p21$^{Waf1/Cip1}$* expression strikingly increased in the hair bulb and oscillated with a 3-week period correlating with hair follicle cycle progression. Notably, this was accompanied by the expression of p63 but not p53. This approach, together with the analysis of *p21$^{Waf1/Cip1}$* knockout mice, has uncovered a novel role for the *p21$^{Waf1/Cip1}$* gene in hair development. These data illustrate the unique utility of bioluminescence imaging in advancing our understanding of the timing and, hence, likely roles of specific gene expression in higher eukaryotes.

aging | cell cycle | hair cycle | imaging

The founding member of the mammalian cyclin-dependent kinase (CDK) inhibitor family, p21$^{Waf1/Cip1}$, is one of the best characterized transcriptional targets of the p53 tumor suppressor protein (1–4). As a general inhibitor of CDKs, p21$^{Waf1/Cip1}$ prevents phosphorylation of the retinoblastoma tumor suppressor protein (pRb) thereby enhancing its growth suppressive function (2, 3, 5). Thus, p21$^{Waf1/Cip1}$ links the p53 pathway to the pRb pathway, providing a tight security network toward tumor suppression. Indeed, the tumor-suppressive role of p21$^{Waf1/Cip1}$ is well documented in various cell culture studies; up-regulation of the *p21$^{Waf1/Cip1}$* gene expression participates in processes such as DNA damage-induced cell cycle arrest, cellular senescence, and terminal differentiation, each of which may prevent tumor formation (5, 6). However, *in vivo*, the role of p21$^{Waf1/Cip1}$, especially in the context of tumor suppression, remains unclear. For example, mutations in the *p21$^{Waf1/Cip1}$* gene are rarely observed in human cancers (7), and, although the majority of mice lacking the *p53* gene develop spontaneous tumors by 6 months of age (8, 9), mice lacking the *p21$^{Waf1/Cip1}$* gene do not exhibit any predisposition to spontaneous tumor formation (10, 11). These observations raise a question of whether the results seen in cell culture truly reflect the physiological roles of p21$^{Waf1/Cip1}$ *in vivo*. However, because knockout experiments performed to date have used mice with germ-line deficiencies at the *p21$^{Waf1/Cip1}$* gene locus, there is the possibility of developmental compensation, as seen with other cell cycle regulators (12, 13). Moreover, expression of the *p21$^{Waf1/Cip1}$* gene overlaps with that of other CDK inhibitor family members in many different tissues (5). It is, therefore, possible that the effects of *p21$^{Waf1/Cip1}$* deficiency is somewhat compromised by developmental or somatic compensation by functionally related CDK inhibitors in *p21$^{Waf1/Cip1}$* knockout mice. Alternative approaches are therefore needed to supplement the *in vitro* studies and assist in understanding the physiological roles of *p21$^{Waf1/Cip1}$* gene expression *in vivo*.

Bioluminescence imaging (BLI) is an emerging approach that is based on detection of light emission from cells or tissues (14, 15). Optical imaging by bioluminescence allows a noninvasive and real-time analysis of various biological responses, such as gene expression, proteolytic processing, or protein–protein interactions, in living animals (16–20). In this study, we generated a transgenic mice line (p21-*p*-luc) expressing the firefly luciferase under the control of the *p21$^{Waf1/Cip1}$* gene promoter. Using this mouse model, we explored the dynamics of *p21$^{Waf1/Cip1}$* gene expression in many different biological processes *in vivo*. This approach, in conjunction with the analysis of *p21$^{Waf1/Cip1}$* knockout mice, uncovered a previously uncharacterized function of *p21$^{Waf1/Cip1}$* gene expression in hair development. The ability to image *p21$^{Waf1/Cip1}$* gene expression noninvasively therefore provides a valuable tool for studies on the role of *p21$^{Waf1/Cip1}$* gene expression *in vivo*.

Results

To study how *p21$^{Waf1/Cip1}$* gene expression is regulated *in vivo*, we attempted to visualize the transcriptional activity of the *p21$^{Waf1/Cip1}$* gene in living animals. To this end, a transgenic mice line (p21-*p*-luc mice) expressing the firefly luciferase

Author contributions: N.O. and Y.I. contributed equally to this work; N.O. and E.H. designed research; N.O., Y.I., K.Y., F.H., R.N., Y.K., N.I., A.T., A.H., and T.S. performed research; N.O., D.J.M., H.S., Y.H., S.A., M.M., K.N., and E.H. analyzed data; and N.O. and E.H. wrote the paper.

The authors declare no conflict of interest.

Freely available online through the PNAS open access option.

Abbreviations: CDK, cyclin-dependent kinase; pRb, retinoblastoma tumor suppressor protein; BLI, bioluminescence imaging.

†To whom correspondence may be addressed. E-mail: ohtani@genome.tokushima-u.ac.jp or hara@genome.tokushima-u.ac.jp.

This article contains supporting information online at www.pnas.org/cgi/content/full/0706949104/DC1.

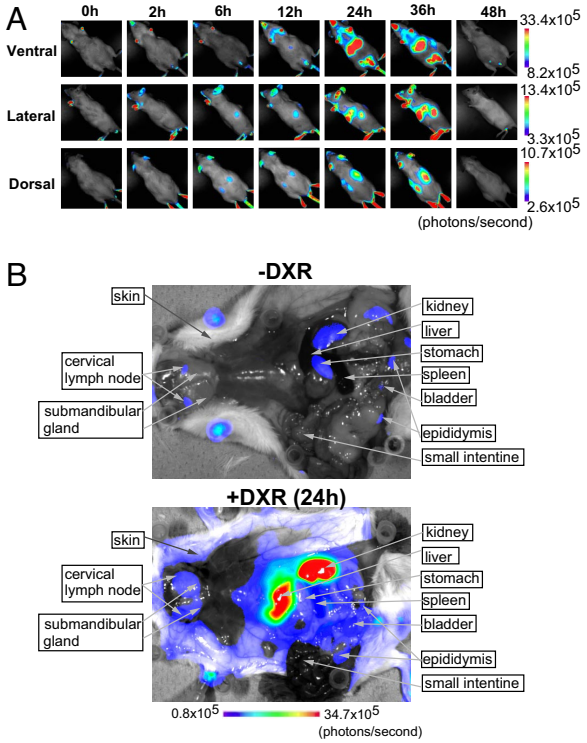

Fig. 1. Characterization of the p21-*p*-luc mice. (*A*) The p21-*p*-luc mice (8-week-old) were injected i.p. with doxorubicin (DXR) (20 mg/kg) and were subjected to noninvasive BLI at various times after doxorubicin (DXR) injection. Representative images of five different experiments are shown. (*B*) The same line of p21-*p*-luc mice were treated with doxorubicin (+DXR) (20 mg/kg) or saline (−DXR) for 24 h, injected with luciferin, and incised through the mouth and anus under anesthesia. Representative BLI data of five different experiments are shown. The color bar indicates photons with minimum and maximum threshold values.

driven by the $p21^{Waf1/Cip1}$ gene promoter, which contains two p53-binding sites, was established and subjected to noninvasive *in vivo* BLI. Although basal levels of bioluminescent signals were very low throughout the body, except for the paws, a striking increase in signal was observed (particularly over the abdomen) within 24 h of treatment with doxorubicin, a DNA damaging agent that activates p53 (Fig. 1*A*). These signals were sustained until 36 h and then declined to baseline values within the next 12 h (Fig. 1*A*, 48 h). To define the organs expressing high levels of luciferase activity, the same lines of transgenic mice were treated with or without doxorubicin for 24 h, injected with luciferin, and incised through mouth and anus under anesthesia (Fig. 1*B*). As expected from noninvasive BLI data (Fig. 1*A*, 24 h), a significant induction of bioluminescent signal was observed in liver and kidney in doxorubicin-treated mice [Fig. 1*B* and supporting information (SI) Fig. 4*A*]. A substantial but less pronounced induction was observed in the submandibular gland, spleen, bladder, and stomach (Fig. 1*B* and SI Fig. 4*A*). Similar but different dynamics of $p21^{Waf1/Cip1}$ gene expression was observed by x-ray irradiation (SI Fig. 5). Importantly, the levels of bioluminescent signal were well correlated with those of endogenous $p21^{Waf1/Cip1}$ mRNA (SI Figs. 4 and 5), indicating that, in the p21-*p*-luc mice, luciferase expression accurately reports the transcriptional dynamics of $p21^{Waf1/Cip1}$ gene expression *in vivo*. Furthermore, in concordance with the levels of endogenous $p21^{Waf1/Cip1}$ expression, luciferase activity was strikingly increased in the cortex and medulla of the kidney (SI Fig. 6). Taken together, these results suggest that the p21-*p*-luc mice provide an ideal tool for the analysis of $p21^{Waf1/Cip1}$ gene expression *in vivo*.

Although p53 serves the beneficial function of tumor suppression, p53 activation may, in some circumstance, act in a manner detrimental to the long-term homeostasis of living organism (21). Indeed, aberrant activation of p53 is known to accelerate the aging process in mice, and the induction of $p21^{Waf1/Cip1}$ gene expression has been shown to be involved this process (22, 23). We thus next attempted to explore the dynamics of $p21^{Waf1/Cip1}$ gene expression throughout entire life span in p21-*p*-luc mice (SI Fig. 7). Unexpectedly, only a slight (3- to 4-fold) induction of bioluminescent signal was observed in aged kidney but not in other aged organs or tissues (SI Fig. 7). Surprisingly, moreover, any signs of strong activation of p53 and DNA damage responses were not observed in aged kidney (SI Fig. 7), indicating that the induction of $p21^{Waf1/Cip1}$ gene expression in aged kidney is likely to be regulated by a p53-independent mechanism, although we cannot rule out the possibility that weak activation of p53 contributes to the up-regulation of $p21^{Waf1/Cip1}$ gene expression.

The up-regulation of $p21^{Waf1/Cip1}$ gene expression is implicated in cellular senescence, the state of stable cell cycle arrest provoked by diverse stresses including DNA damage and oncogenic *ras* expression in cultured primary cells (4, 24). To explore this notion *in vivo*, p21-*p*-luc mice were subjected to a conventional chemically induced skin tumor protocol with a single dose of DMBA for initiation and biweekly treatment with 12-*o*-tetradecanoylphorbol 13-acetate (TPA) for promotion. Because this protocol causes an oncogenic mutation in the H-*ras* gene, it appeared to be ideal for studying physiological responses against oncogenic *ras* expression in living animals (25, 26). In agreement with previous reports (25, 26), benign skin papillomas began to appear after 7–8 weeks of promotion (Fig. 2*A*). Notably, papilloma formation was accompanied by the induction of a bioluminescence signal (Fig. 2*A*), endogenous $p21^{Waf1/Cip1}$ expression, and activation of p53 (Fig. 2*B*). These observations, together with previous studies that indicate that disruption of the $p21^{Waf1/Cip1}$ gene results in an increase of papilloma formation or carcinoma formation (27–29), strongly suggest that $p21^{Waf1/Cip1}$ plays a preventative role against oncogenic *ras*-signaling *in vivo*.

Because noninvasive BLI permits continuous readout of gene expression in living animals (14, 15), we next examined the kinetics of $p21^{Waf1/Cip1}$ gene expression toward papilloma formation. To our surprise, a remarkable bioluminescent signal was observed well before papilloma appearance and oscillated with a 3-week period (Figs. 2 *C* and *D*). Unexpectedly, moreover, a remarkable expression of endogenous $p21^{Waf1/Cip1}$ was observed in the hair bulb, but not in the skin itself (Fig. 2*E*), suggesting that $p21^{Waf1/Cip1}$ may play a role in hair development. To produce new hairs, existing hair follicles undergo cycles of growth (anagen), regression (catagen), and rest (telogen) (30). Because TPA treatment has been shown to promote entry of hair follicles into their anagen phase (31), we next asked whether the oscillating bioluminescence signal in DMBA/TPA-treated skin reflects hair follicle cycle progression. Although TPA treatment, in itself, did not cause skin papilloma formation, a similar oscillation of bioluminescence signals and $p21^{Waf1/Cip1}$ mRNA expression was induced by TPA treatment alone (SI Fig. 8). Notably, this was accompanied by remarkable hair growth (SI Fig. 8*A*), suggesting a role for $p21^{Waf1/Cip1}$ in the hair follicle cycle progression in mouse skin.

To substantiate this idea in a more physiological setting, we next tested whether $p21^{Waf1/Cip1}$ expression oscillates throughout the natural hair follicle cycle, exploiting the fact that hair follicle cycles are synchronized for the first two postnatal periods of hair follicle growth in mice (32). Although the dynamics of hair cycle progression were visually undetectable during the second postnatal hair follicle cycle, BLI was sensitive enough to monitor oscillating $p21^{Waf1/Cip1}$ expression (Fig. 3*A*). The levels of biolu-

GENETICS

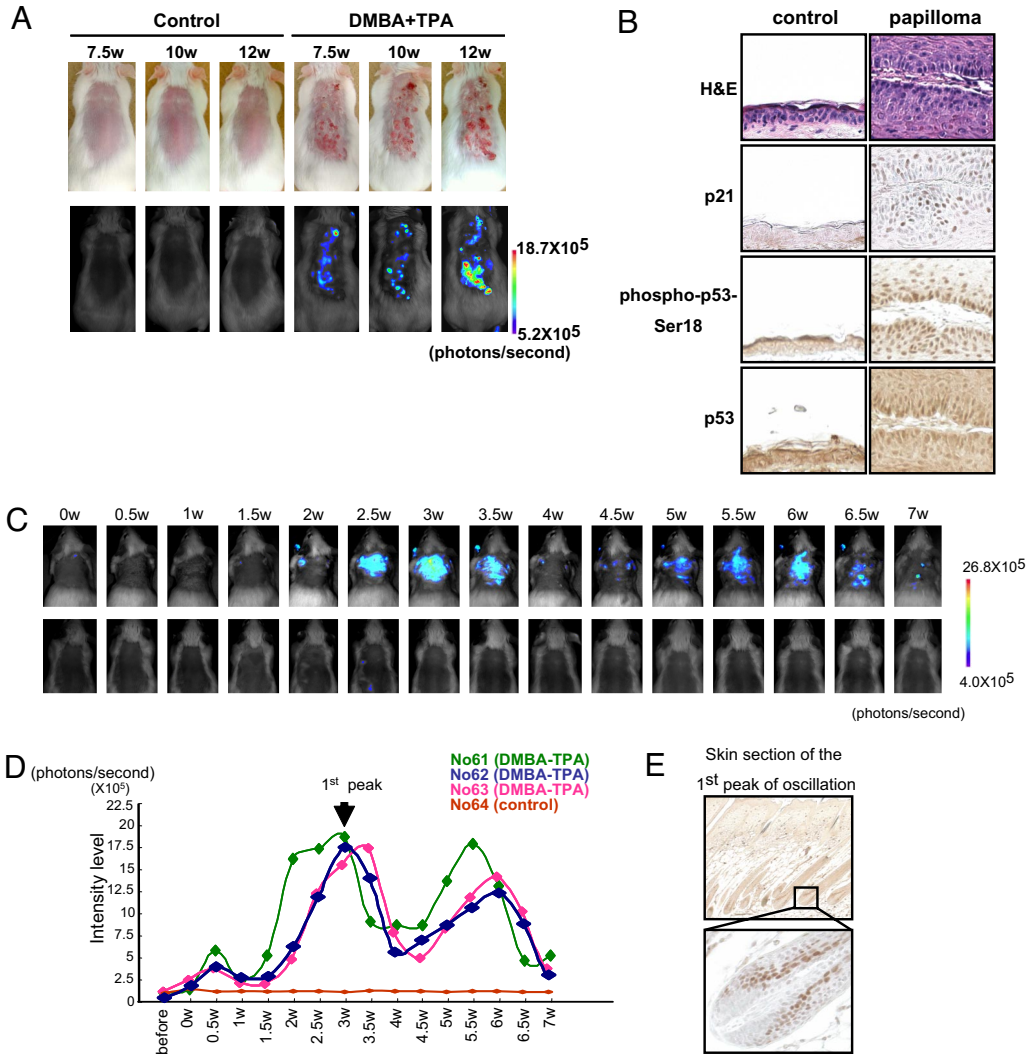

Fig. 2. Oscillation of bioluminescence signals in DMBA/TPA-treated mouse skin. (*A*) The p21-*p*-luc mice treated with DMBA/TPA or with acetone (control) were subjected to noninvasive BLI at indicated time points after TPA treatment. Representative images of 12 different experiments were shown (*Lower*). These papillomas and control skin were photographed in regular lighting (*Upper*). The color bar indicates photons with minimum and maximum threshold values. (*B*) H&E staining and the immunohistochemistry for endogenous $p21^{Waf1/Cip1}$ expression, phosphorylation of p53 at serine 18 residue, and p53 expression were performed by using biopsy samples of skin papilloma (*Right*) or control normal skin (*Left*). (*C*) Noninvasive BLI was performed throughout the time course after DMBA/TPA treatment (*Upper*) or acetone control (*Lower*). Mice were imaged at 0.5-week intervals after TPA treatment. Representative images of 12 different experiments were shown. The color bar indicates photons with minimum and maximum threshold values. (*D*) The intensity of bioluminescence signal throughout the time course was graphed. (*E*) Immunohistochemistry was conducted to examine the endogenous $p21^{Waf1/Cip1}$ expression in the dorsal skin at 3 weeks after TPA treatment (corresponding to the first peak of bioluminescence oscillation). A magnified image of hair bulb is shown (*Lower*).

minescence signals reached their peak at postnatal day 28 (P28); endogenous $p21^{Waf1/Cip1}$ expression was also strongly observed in the precortex area above the hair matrix (differentiating cell area) at this time (Fig. 3*A*). These data suggest that $p21^{Waf1/Cip1}$ may regulate the size of hair bulb and thereby control the hair phenotype.

To explore this possibility, microscopic examination of the various hair types was conducted by using mice with different $p21^{Waf1/Cip1}$ genotypes (10). The morphology of the four main hair types (guard, awl, auchene, and zigzag) was not significantly different among three different genotypes ($p21^{+/+}$, $p21^{+/-}$, $p21^{-/-}$) (data not shown). However, the proportion of zigzag hairs, which are produced by the smallest hair bulb, was significantly reduced in $p21^{+/-}$ mice, whereas awl hairs and auchene hairs, which are produced by the intermediate-sized hair bulb, were increased (Fig. 3*B*). Curiously, these effects were less pronounced in $p21^{-/-}$ mice (Fig. 3*B*). Importantly, however, unusually high level of $p27^{Kip1}$ expression, another member of the $p21^{Waf1/Cip1}$ family CDK inhibitors, was observed in the hair bulb of $p21^{-/-}$ mice (Fig. 3*C*). Thus, it is likely that the effects of $p21^{Waf1/Cip1}$ deficiency are concealed, at least in part, by up-regulation of $p27^{Kip1}$ expression in the hair bulb of $p21^{-/-}$ mice. In line with this observation, the proportion of zigzag hairs has been shown to reduce in $p27^{Kip1}$ knockout mice (33), suggesting that $p21^{Waf1/Cip1}$ and $p27^{Kip1}$ possess overlapping role(s) in hair development.

It is worthwhile to note that a similar level of $p21^{Waf1/Cip1}$ expression was observed in anagen hair bulbs, regardless of p53 gene status (SI Fig. 9*A*). Moreover, the proportion of four main hair types was not substantially different among mice of three different genotypes ($p53^{+/+}$, $p53^{+/-}$, $p53^{-/-}$) (SI Fig. 9*B*), suggesting that p53 is not a major player in this setting. Interestingly, although we were unable to see any p53 expression in the hair bulb throughout hair follicle cycle (data not shown), the levels of

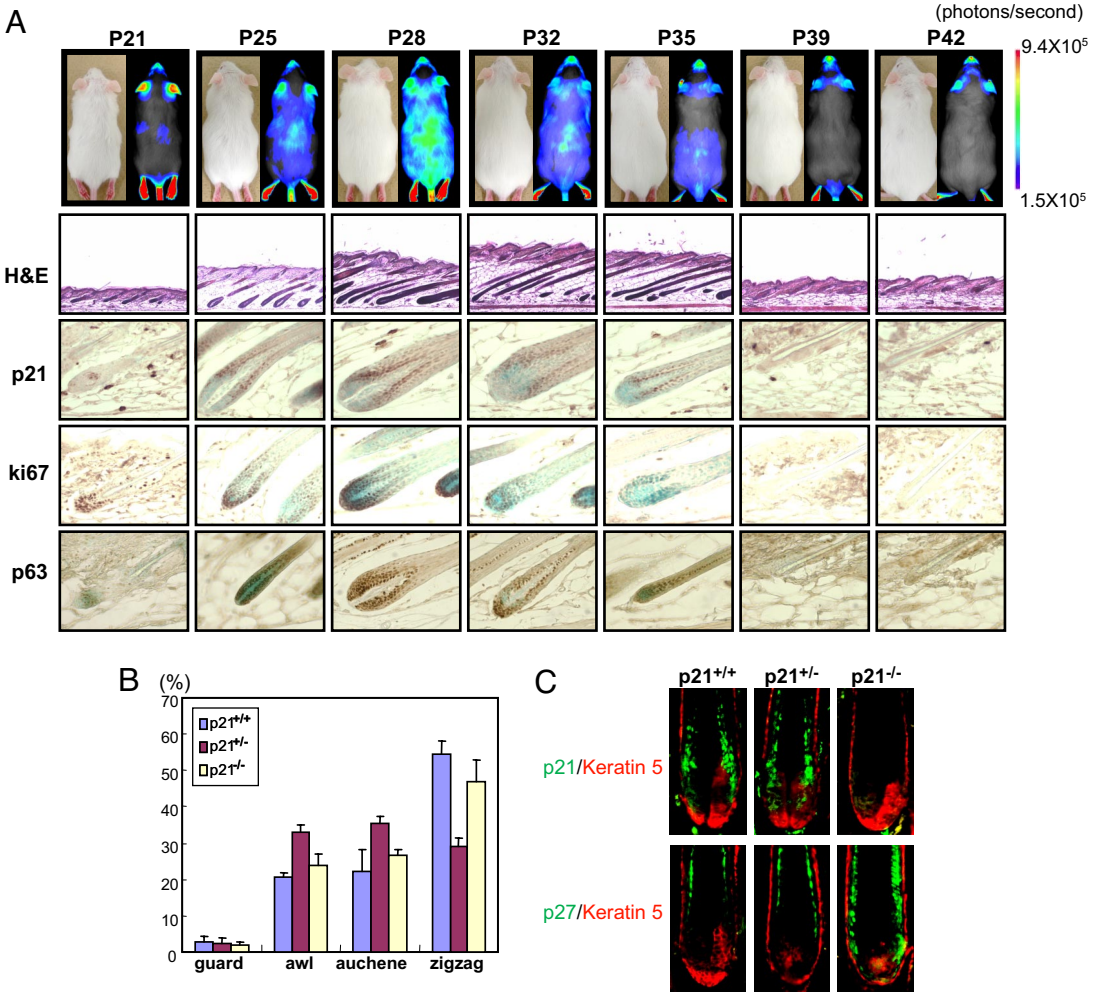

Fig. 3. Real-time imaging of hair follicle cycle oscillation in living mice. (*A*) The p21-*p*-luc mice were subjected to noninvasive BLI from postnatal day 21 (P21) to P42. Representative images of five different experiments are shown at the top. The color bar indicates photons with minimum and maximum threshold values. At the indicated time point of postnatal development, dorsal skin of p21-*p*-luc mice was harvested and processed for H&E staining or for immunohistochemistry. (*B*) Summary of the prevalence of hair phenotypes in mice of different $p21^{Waf1/Cip1}$ genotype (C57BL/6 background). The means ± SD of three independent experiments are shown. (*C*) Immunofluorescence of dorsal skin section from P28 mice was performed by using antibodies against $p21^{Waf1/Cip1}$ (green) or $p27^{Kip1}$ (green). Keratin 5 (red) was used as a marker for outer root sheath.

p63 (34), a member of p53-family of transcription factors, were dramatically increased in anagen hair bulbs (Fig. 3*A*). Together, these results imply that p63, but not p53, may play a critical role in the regulation of hair development.

Discussion

In this study, we generated a transgenic mouse model to visualize $p21^{Waf1/Cip1}$ gene expression in living animals. The p21-*p*-luc mice carry the firefly luciferase cDNA under the control of the $p21^{Waf1/Cip1}$ gene promoter. Because this promoter contains two canonical p53-binding sites, this mouse model is expected to be an ideal system for monitoring not only $p21^{Waf1/Cip1}$ gene expression, but also p53 activation *in vivo*. Indeed, a dramatic induction of bioluminescent signal was observed in various organs within 24 h upon treatment with doxorubicin, a well known DNA-damaging agent that activates p53 (Fig. 1 and SI Fig. 4). Notably, different dynamics of $p21^{Waf1/Cip1}$ gene expression were observed when p21-*p*-luc mice were irradiated with x-ray (SI Fig. 5). In both cases, the levels of bioluminescent signals observed were well correlated with those of endogenous $p21^{Waf1/Cip1}$ mRNA detected by RT-PCR analysis (Fig. 1 and SI Figs. 4 and 5), indicating that the p21-*p*-luc mice provide an ideal tool to monitor the expression of $p21^{Waf1/Cip1}$ gene and/or activity of p53 in living animals. Interestingly, neither doxorubicin nor x-rays induced $p21^{Waf1/Cip1}$ gene expression in the small intestine, implying that p53 is not a major regulator of $p21^{Waf1/Cip1}$ gene expression in the small intestine, as suggested by previous studies (35).

By monitoring and quantifying $p21^{Waf1/Cip1}$ gene expression repeatedly in the same mouse throughout its entire life span, we revealed the dynamics of $p21^{Waf1/Cip1}$ gene expression during the aging process in living mice. Only a slight (3- to 4-fold) induction of bioluminescent signal was observed in kidney, but not in other organs, as mice age (SI Fig. 7). Moreover, strong signs of p53 activation and DNA damage responses were virtually undetectable in aged kidney (SI Fig. 7). These results were unexpected because several lines of evidence suggest that p53-dependent induction of $p21^{Cip1/Waf1}$ is involved in the aging process (22, 23, 36). Our results are, however, consistent with a recent RT-PCR-based study showing that only a slight increase in the $p21^{Waf1/Cip1}$ gene expression was seen in tissues from old mice versus young mice (37, 38). Moreover, it has been shown that increased p53 expression under the endogenous p53 gene promoter protects mice from tumorigenesis without showing any indication of

accelerated aging (39). Furthermore, $p21^{Waf1/Cip1}$ appears to play protective effects on stem cell exhaustion and ionizing radiation, which may underlie the long-term homeostasis throughout entire life span (40–42). Thus, it is likely that the role of $p21^{Waf1/Cip1}$ in organismal aging is context-dependent and more complicated than envisaged.

Another important aspect of the p53/$p21^{Waf1/Cip1}$ pathway is the induction of cellular senescence (4, 24), the state of permanent cell cycle arrest provoked by a variety of oncogenic stimuli including oncogenic *ras* expression in cultured primary cells (43–45). Because this mechanism is poorly understood *in vivo* (46), we tested this notion using our *in vivo* BLI system. Indeed, DMBA/TPA treatment, which causes an oncogenic mutation of the endogenous H-*ras* gene (25, 26), resulted in a significant induction of $p21^{Waf1/Cip1}$ expression accompanied by skin papilloma formation (Fig. 2*A*). Because the induction of $p21^{Waf1/Cip1}$ expression can be seen from the very beginning of papilloma formation and was further enhanced as the papillomas developed (Fig. 2*A*), the $p21^{Waf1/Cip1}$ gene is likely to play multiple roles in preventing benign skin papilloma formation and/or malignant conversion. These results are somewhat consistent with two conflicting reports; one shows that disruption of the $p21^{Waf1/Cip1}$ gene accelerates benign skin papilloma formation but not malignant conversion (27), and the other shows that disruption of the $p21^{Waf1/Cip1}$ gene accelerates malignant conversion but not benign skin papilloma formation (28).

During the time-course BLI experiments in skin tumor formation, we unexpectedly found that the expression of $p21^{Waf1/Cip1}$ oscillates over the 3-week time course of the hair follicle cycle (Figs. 2 *C* and *D* and 3*A*). Moreover, although the morphology of the four main hair types was not remarkably different, the proportion of zigzag hairs, which are produced by the smallest hair bulb, was significantly reduced in $p21^{+/-}$ mice (Fig. 3*B*). Surprisingly, the effects of $p21^{Waf1/Cip1}$ deficiency were less pronounced in $p21^{-/-}$ mice than in heterozygotes (Fig. 3*B*) because of an up-regulation of $p27^{Kip1}$ expression in the hair bulb of $p21^{-/-}$ mice (Fig. 3*C*). In concordance with this notion, recent study revealed that the proportion of zigzag hairs is substantially reduced in mice lacking $p27^{Kip1}$ (33) Thus, there is cross-talk between $p21^{Waf1/Cip1}$ and $p27^{Kip1}$ in controlling hair phenotype. Note that the proportion of zigzag hairs is also reduced in mice lacking the *Sox18* gene (47), and Sox family transcription factors are known to activate $p21^{Waf1/Cip1}$ expression (48). Thus, it is tempting to speculate that Sox18 controls hair phenotype through regulating $p21^{Waf1/Cip1}$ gene expression in the hair bulb. It is also important to note, however, that the expression of p63 (34), a member of p53 family transcription factor, overlapped with that of $p21^{Waf1/Cip1}$ in the hair bulb (Fig. 3*A*). It is therefore likely that $p21^{Waf1/Cip1}$ gene expression is controlled by multiple factors in hair bulbs.

We are currently uncertain about the biological consequence of alteration of the zigzag hair proportion in $p21^{+/-}$ mice. However, because the hair coat plays a crucial role in controlling body temperature in the wild, it is interesting to speculate that $p21^{Waf1/Cip1}$ and/or $p27^{Kip1}$ may be involved in temperature control in the wild. Taken together, our results reveal an unexpected role for $p21^{Waf1/Cip1}$ and provide an insight into how the hair phenotype is determined. Visualizing the dynamics of $p21^{Waf1/Cip1}$ gene expression in living mice, therefore, provides a powerful tool for not only help to resolve and clarify issues connecting *in vitro* studies but also reveals unrecognized functions of this key proliferative regulator in various physiological processes *in vivo*.

Materials and Methods

Generation of p21-*p*-luc transgenic mouse. The 2.5-kb fragment of the $p21^{Waf1/Cip1}$ gene promoter containing two p53-binding sites (GenBank accession number: NW_923073.1; from 9663447 to 9665888) was placed in front of the firefly luciferase reporter cDNA in the pGL3-basic plasmid vector (Promega, Madison, WI) (see plasmid construction map in SI Fig. 10). The plasmid DNA was digested with XhoI and SalI, and the DNA fragment containing the $p21^{Waf1/Cip1}$ gene promoter, luciferase cDNA, and polyA signal was isolated and used for microinjection. The transgenic mouse strain was generated by pronuclear microinjection of the reporter transgene into fertilized CD1 oocytes. Genotyping of transgenic mice was determined by PCR and was confirmed by whole-body BLI. One transgenic line, #34 (CDB0415T-34), was selected for studies described in this article because the levels of bioluminescence signals were well correlated with those of endogenous $p21^{Waf1/Cip1}$ mRNA. All animals were cared for by using protocols approved by the Committee for the Use and Care of Animals of the University of Tokushima.

Bioluminescence Imaging. For the detection of luciferase expression, mice were anesthetized, injected i.p. with D-luciferin sodium salt (75 mg/kg) 5 min before beginning photon recording (16–20). Mice were placed in the light-tight chamber, and a gray-scale image of the mice was first recorded with dimmed light, followed by acquisition of luminescence image by using a cooled CCD camera (Princeton Instruments, Trenton, NJ). The signal-to-noise ratio was increased by 2×2 binning and 5 min exposure, unless otherwise stated in the text. For colocalization of the luminescent photon emission on the animal body, gray scale and pseudocolor images were merged by using IMAGE-PRO PLUS (Media Cybernetics, Bethesda, MD).

Tumor-Induction Experiments. Twelve mice of the p21-*p*-luc line, in the resting phase of the hair cycle (8-week-old), were shaved and treated with 7,12-dimethylbenzanthracene (DMBA) (100 μg in 100 μl of acetone). One week after DMBA treatment, mice were subsequently treated twice a week with TPA (12.5 μg in 100 μl of acetone) for 20 weeks (25, 26). Control mice were treated with acetone instead of DMBA/TPA.

Semiquantitative RT-PCR. Total RNA was isolated by using TRIzol reagent (Invitrogen, Carlsbad, CA), and 2 μg of total RNA was used for the reverse-transcriptase reaction. The PCR was performed by using Blend Taq polymerase (TOYOBO, Osaka, Japan) with primers specific for the mouse $p21^{Waf1/Cip1}$ gene and the mouse β-*actin* gene. The PCR primer sequences used are shown in *SI Text*.

Real-Time RT-PCR. Quantitative real-time RT-PCR was performed by using the SYBER Premix EX Taq system (TAKARA, Otsu, Japan) and an ABI Prism 7900HT (Applied Biosystems, Foster City, CA). Amplified signals were confirmed to be single bands by gel electrophoresis and were normalized to the levels of GAPDH. Data were analyzed by using SDS2.1 software (Applied Biosystems). The PCR primer sequences used are shown in *SI Text*.

Histology and Immunohistochemistry. Biopsies of mouse skin taken from the middorsal region were fixed in 10% formalin for a 24 h or longer, progressively dehydrated through gradients of alcohol, and embedded in paraffin. Samples were sectioned on a microtome (5-μm-thick), deparaffinized in xylene, rehydrated, and then stained with hematoxylin and eosin (H&E). The hair cycle status was determined by histological examination. For antibody staining, deparaffinized and rehydrated sections were exposed to heat-induced antigen retrieval for 5 min or 20 min in 10 mM citrate buffer (pH 6.0). After washing in PBS, endogenous peroxidase activity was quenched for 15 min in 1% H_2O_2 in methanol, followed by washing with PBS. The sections were

incubated in blocking serum for 1 h at room temperature. After incubation with primary antibodies overnight at 4°C, biotinylated anti-mouse secondary antibody was applied and detected by the avidin–biotin peroxidase technique using the DAB kit (DAKO, Glostrup, Denmark) and then counterstained with methyl green. For immunofluorescence, the relevant Alexa Fluor 488 goat anti-mouse or 546 goat anti-rabbit antibodies (1:1,000; Invitrogen) were used for detection of primary antibodies. Fluorescence images were observed and photographed by using an immunofluorescence microscope (Carl Zeiss, Oberkochen, Germany). The primary antibodies used are shown in *SI Text*.

Hair Measurements. Hair was removed from the middorsal region of each mouse (8-week-old) to reduce the potential regional variation, although this is not known to occur in the dorsal region of the mouse. One hundred hairs were examined to determine the percentage of each hair type.

We thank Dr. P. Leder (Department of Genetics, Harvard Medical School, Boston, MA) for providing $p21^{Waf1/Cip1}$ knockout mice. We also thank Ms. S. Chiba for her assistance in various mouse experiments. This work was supported by grants from Ministry of Education, Science, Sports, and Culture of Japan, the Astellas Foundation for Research on Metabolic Disorders and the Astellas Foundation for Research on Medical Resources.

1. El-Deiry WS, Tokino T, Velculescu VE, Levy DB, Parsons R, Trent JM, Lin D, Mercer WE, Kinzler KW, Vogelstein B (1993) *Cell* 75:817–825.
2. Harper JW, Adami GR, Wei N, Keyomarsi K, Elledge SJ (1993) *Cell* 75:805–816.
3. Xiong Y, Hannon GJ, Zhang H, Casso D, Kobayashi R, Beach D (1993) *Nature* 366:701–704.
4. Noda A, Ning Y, Venable SF, Pereira-Smith OM, Smith JR (1994) *Exp Cell Res* 211:90–98.
5. Sherr CJ, Roberts JM (1999) *Genes Dev* 13:1501–1512.
6. Rowland BD, Peeper DS (2006) *Nat Rev Cancer* 6:11–23.
7. El-Deiry WS (1998) *Curr Top Microbiol Immunol* 227:121–137.
8. Donehower LA, Harvey M, Slagle BL, McArthur MJ, Montgomery CA, Jr, Butel JS, Bradley A (1992) *Nature* 356:215–221.
9. Jacks T, Remington L, Williams BO, Schmitt EM, Halachmi S, Bronson RT, Weinberg RA (1994) *Curr Biol* 4:1–7.
10. Deng C, Zhang P, Harper JW, Elledge SJ, Leder P (1995) *Cell* 82:675–684.
11. Brugarolas J, Chandrasekaran C, Gordon JI, Beach D, Jacks T, Hannon GJ (1995) *Nature* 377:552–557.
12. Sage J, Mulligan GJ, Attardi LD, Miller A, Chen S, Williams B, Theodorou E, Jacks T (2000) *Genes Dev* 14:3037–3050.
13. Ciemerych MA, Kenney AM, Sicinska E, Kalaszczynska I, Bronson RT, Rowitch DH, Gardner H, Sicinski P (2002) *Genes Dev* 16:3277–3289.
14. Contag PR, Olomu IN, Stevenson DK, Contag CH (1998) *Nat Med* 4:245–247.
15. Gross S, Piwnica-Worms D (2005) *Cancer Cell* 7:5–15.
16. Uhrbom L, Nerio E, Holland EC (2004) *Nat Med* 10:1257–1260.
17. Zhang GJ, Safran M, Wei W, Sorensen E, Lassota P, Zhelev N, Neuberg DS, Shapiro G, Kaelin WG, Jr (2004) *Nat Med* 10:643–648.
18. Li F, Sonveaux P, Rabbani ZN, Liu S, Yan B, Huang Q, Vujaskovic Z, Dewhirst MW, Li CY (2007) *Mol Cell* 26:63–74.
19. Vooijs M, Jonkers J, Lyons S, Berns A (2002) *Cancer Res* 62:1862–1867.
20. Paulmurugan R, Umezawa Y, Gambhir SS (2002) *Proc Natl Acad Sci USA* 99:15608–15613.
21. Sharpless NE, DePinho RA (2002) *Cell* 110:9–12.
22. Tyner SD, Venkatachalam S, Choi J, Jones S, Ghebranious N, Igelmann H, Lu X, Soron G, Cooper B, Brayton C, *et al.* (2002) *Nature* 415:45–53.
23. Maier B, Gluba W, Bernier B, Turner T, Mohammad K, Guise T, Sutherland A, Thorner M, Scrable H (2004) *Genes Dev* 18:306–319.
24. Serrano M, Lin AW, McCurrach ME, Beach D, Lowe SW (1997) *Cell* 88:593–602.
25. Quintanilla M, Brown K, Ramsden M, Balmain A (1986) *Nature* 322:78–80.
26. Kemp CJ (2005) *Semin Cancer Biol* 15:460–473.
27. Weinberg WC, Fernandez-Salas E, Morgan DL, Shalizi A, Mirosh E, Stanulis E, Deng C, Hennings H, Yuspa SH (1999) *Cancer Res* 59:2050–2054.
28. Topley GI, Okuyama R, Gonzales JG, Conti C, Dotto GP (1999) *Proc Natl Acad Sci USA* 96:9089–9094.
29. Oskarsson T, Essers MA, Dubois N, Offner S, Dubey C, Roger C, Metzger D, Chambon P, Hummler E, Beard P, Trumpp A (2006) *Genes Dev* 20:2024–2029.
30. Fuchs E (2007) *Nature* 445:834–842.
31. Flores I, Cayuela ML, Blasco MA (2005) *Science* 309:1253–1256.
32. Sarin KY, Cheung P, Gilison D, Lee E, Tennen RI, Wang E, Artandi MK, Oro AE, Artandi SE (2005) *Nature* 436:1048–1052.
33. Sharov AA, Sharova TY, Mardaryev AN, Tommasi di Vignano A, Atoyan R, Weiner L, Yang S, Brissette JL, Dotto GP, Botchkarev VA (2006) *Proc Natl Acad Sci USA* 103:18166–18171.
34. Senoo M, Pinto F, Crum CP, McKeon F (2007) *Cell* 129:523–536.
35. Macleod KF, Sherry N, Hannon G, Beach D, Tokino T, Kinzler K, Vogelstein B, Jacks T (1995) *Genes Dev* 9:935–944.
36. Choudhury AR, Ju Z, Djojosubroto MW, Schienke A, Lechel A, Schaetzlein S, Jiang H, Stepczynska A, Wang C, Buer J, *et al.* (2007) *Nat Genet* 39:99–105.
37. Krishnamurthy J, Torrice C, Ramsey MR, Kovalev GI, Al-Regaiey K, Su L, Sharpless NE (2004) *J Clin Invest* 114:1299–1307.
38. Edwards MG, Anderson RM, Yuan M, Kendziorski CM, Weindruch R, Prolla TA (2007) *BMC Genomics* 8:80.
39. Garcia-Cao I, Garcia-Cao M, Martin-Caballero J, Criado LM, Klatt P, Flores JM, Weill JC, Blasco MA, Serrano M (2002) *EMBO J* 21:6225–6235.
40. Cheng T, Rodrigues N, Shen H, Yang Y, Dombkowski D, Sykes M, Scadden DT (2000) *Science* 287:1804–1808.
41. Kippin TE, Martens DJ, van der Kooy D (2005) *Genes Dev* 19:756–767.
42. Wang YA, Elson A, Leder P (1997) *Proc Natl Acad Sci USA* 94:14590–14595.
43. Gil J, Peters G (2006) *Nat Rev Mol Cell Biol* 7:667–677.
44. Campisi J (2005) *Cell* 120:513–522.
45. Takahashi A, Ohtani N, Yamakoshi K, Iida S, Tahara H, Nakayama K, Nakayama KI, Ide T, Saya H, Hara E (2006) *Nat Cell Biol* 8:1291–1297.
46. Narita M, Lowe SW (2005) *Nat Med* 11:920–922.
47. Pennisi D, Bowles J, Nagy A, Muscat G, Koopman P (2000) *Mol Cell Biol* 20:9331–9336.
48. Panda DK, Miao D, Lefebvre V, Hendy GN, Goltzman D (2001) *J Biol Chem* 276:41229–41236.